Impact Factor:					
	ISRA (India) = 6.317	SIS (USA) = 0.912	ICV (Poland) = 6.630
	ISI (Dubai, UAE) = 1.582	РИНЦ (Russia) = 0.126	PIF (India) = 1.940
	GIF (Australia) = 0.564	ESJI (KZ) = 9.035	IBI (India) = 4.260
	JIF = 1.500	SJIF (Morocco) = 7.184	OAJI (USA) = 0.350

SOI: 1.1/TAS DOI: 10.15863/TAS

International Scientific Journal

Theoretical & Applied Science

p-ISSN: 2308-4944 (print) **e-ISSN:** 2409-0085 (online)

Year: 2021 **Issue:** 06 **Volume:** 98

Published: 14.06.2021 **http://T-Science.org**

QR – Issue QR – Article

Rashid Nietalievich Jaksibaev
Tashkent institute of irrigation and agricultural mechanization engineers
Doctoral Candidate
Tashkent, Uzbekistan
r.jaksibaev@tiiame.uz

Sabit Nietalievich Gabbarov
Nukus branch of the Navoi State Mining and Metallurgical Institute
Senior lecturer
Nukus, Uzbekistan
gabbarovs@mail.ru

GEOINFORMATIONAL ANALYSIS OF THE NEGATIVE EFFECTS OF THE ARAL SEA ON PASTURES

Abstract: *The Aral Sea has been drying up for years. As a result, sandy areas appear in the dry part of the Aral Sea. This, in turn, has a negative impact on the environment of the regions of the Aral Sea. This article examines the negative impact of the drying up of the Aral Sea on the Aral Sea region. Areas from the Ustyurt Plateau and the Amudarya Delta were selected and analyzed. Data were taken from Landsat 8 and calculated in eCognation based on special algorithms and formulas, and the images were processed in ArcGIS. The research was conducted on a seasonal basis in two selected regions as of 2020. In the research identified NDVI, NDBI, SI, NDWI, MNDWI, LST indices and learned their interrelationships in the regions. Due to the fact that the selected areas are mainly arid, harsh conditions and desert areas, a geographic information analysis of the use of these lands as pastures was developed.*

Key words: *Remote sensing (RS), Geographic information system (GIS), Normalized difference vegetation index (NDVI), Normalized difference built-up index (NDBI), Bare soil index (BSI), Normalized Difference Water Index (NDWI), Modified Normalized Difference Water Index (MNDWI), Land surface temperature (LST).*

Language: *English*

Citation: Jaksibaev, R. N., & Gabbarov, S. N. (2021). Geoinformational analysis of the negative effects of the Aral Sea on pastures. *ISJ Theoretical & Applied Science, 06 (98)*, 356-362.

Soi: http://s-o-i.org/1.1/TAS-06-98-39 ***Doi***: crossref https://dx.doi.org/10.15863/TAS.2021.06.98.39

Scopus ASCC: *3305.*

Introduction

Pastures are one of the most important types of agricultural land (Norqulov and Sheraliev, 2010, Sultashova et al., 2020). The role of pastures in providing the population with quality milk and dairy products, quality meat products is very important (Parente and Ferreira 2018, Osvaldo et al., 2018). In agriculture, the use of lands with dry and unfavorable climatic conditions mainly as pastures is more effective (Di Bella 2004). This category of land is recommended for grazing sheep and goats, and this category of land is found around the Aral Sea.

One of the most pressing issues in the region is to ensure the efficient use of sandy soils formed as a result of the drying up of the Aral Sea, to reduce and prevent the negative effects of drought (Berdimbetov et al., 2020). To do this, it is necessary to first study the level of impact of the negative consequences by region.

The relationship between natural factors such as vegetation rate, precipitation, and temperature changes in the efficient use of land around the Aral Sea has been extensively studied (Mathew, Stuart 2020, Julianne et al., 2020). It is also important to

study and analyze plant vegetation, land use, water use, soil salinity, and soil temperature levels.

Most of the area is sandy, the climate is dry, variable precipitation is observed mainly in winter and spring, almost no precipitation in summer and autumn, very low snowfall and short-term storage in this area, as well as high evaporation rates in the summer months, it is necessary to study the level of use of these lands as pastures in agriculture.

Study area

The Aral Sea is situated in Central Asia, between the Southern part of Kazakhstan and Northern Uzbekistan (Turdimambetov et al., 2021, Christopher et al., 2020, Izimbet et al., 2020). In selecting the sites for the study, it is advisable to pay special attention to the study of the negative effects of the drying of the Aral Sea on a regional scale. Basically, the selected area on the Ustyurt Plateau is located in the northwestern part of the Aral Sea (X: 541305-579015, Y: 4977345-5003685) and the selected area from the Amudarya delta is in the southeastern part (X: 720135-743655, Y: 4777575-4792425) located. The selected areas are located in the territory of the Republic of Uzbekistan.

During the study, it is advisable to study the lands as natural pastures. In the study of the natural properties of the two regions selected in the study, it is important to implement on the basis of data from Landsat 8 and determine the relationship between NDVI, BSI, NDWI, MNDWI, SI and LST and develop scientifically based recommendations.

Normalized Difference Vegetation Index: (NDVI) quantifies vegetation by measuring the difference between near-infrared and red light. NDVI always ranges from -1 to +1. As shown below, Normalized Difference Vegetation Index uses the NIR and red channels in its formula:

$$NDVI = (NIR-RED)/(NIR+RED); \quad (1)$$

Healthy vegetation (chlorophyll) reflects more near-infrared (NIR) and green light compared to other wavelengths. But it absorbs more red and blue light. Overall, NDVI is a standardized way to measure healthy vegetation. When you have high NDVI values, you have healthier vegetation. When you have low NDVI, you have less or no vegetation (Jaksibaev 2020, gisgeography.com).

Bare Soil Index: BSI is a numerical indicator that combines blue, red, near infrared and short wave infrared spectral bands to capture soil variations. These spectral bands are used in a normalized manner.

BSI is calculated (Nguyen et al., 2021, Sanne et al., 2017):

$$BSI=((SWIR–RED)-(NIR+BLUE))/((SWIR–RED)+(NIR+BLUE)); \quad (2)$$

The Normalized Difference Water Index: NDWI is a remote sensing derived index estimating the leaf water content at canopy level.

NDWI is calculated (Luyan Ji et al., 2015):

$$NDWI=(NIR–SWIR)/(NIR+SWIR); \quad (3)$$

The Modified Normalized Difference Water Index: MNDWI uses green and SWIR bands for the enhancement of open water features. It also diminishes built-up area features that are often correlated with open water in other indices.

MNDWI is calculated (Luyan Ji et al., 2015):

$$MNDWI = (Green – SWIR)/(Green+ SWIR); \quad (4)$$

The Salinity Index: The salinity index measures the direct relationship between Electrical Conductivity (EC) and moisture. This ratio tells you the concentration of salinity in the available moisture. For instance, with moisture being consistent and EC rising, salinity concentration will go up and salinity index will rise.

SI is calculated (Mohamed Elhag 2015):

$$SI=(NIR*RED)/(GREEN) \quad (5)$$

Land Surface Temperature: (LST) is the radiative skin temperature of the land derived from solar radiation. A simplified definition would be how hot the "surface" of the Earth would feel to the touch in a particular location. Land surface temperature is not the same as the air temperature that is included in the daily weather report.

Calculation of LST: The first step of the algorithm is the input of Band 10. After inputting band 10, in the background, the tool uses formulas taken from the USGS web page for retrieving the top of atmospheric (TOA) spectral radiance ($L\lambda$):

$$L\lambda = ML*Q\text{cal} + AL, \quad (6)$$

Where ML represents the band-specific multiplicative rescaling factor, Qcal is the Band 10 image, AL is the band-specific additive rescaling factor.

After the digital numbers (DNs) are converted to reflection, the TIRS band data should be converted from spectral radiance to brightness temperature (BT) using the thermal constants provided in the metadata file. The following equation is used in the tool's algorithm to convert reflectance to BT:

$$BT=(K2/\ln[(K1/L\lambda)+1])-273.15, \quad (7)$$

where, $K1$ and $K2$ stand for the band-specific thermal conversion constants from the metadata.

Next step of the algorithm is NDVI Method for Emissivity Correction. NDVI is calculated from the first equation above. Then we calculate the Proportion of Vegetation. It is calculated as follows:

$$PV = ((NDVI-NDVI_L)/(NDVI_H- NDVI_L))^2, \quad (8)$$

Then land surface emissivity is calculated:

$$\varepsilon = 0.004* PV+0.986, \quad (9)$$

The last step of retrieving the LST or the emissivity corrected land surface temperature T_s is computed as follows (Jaksibaev 2020, Avdan and Jovanovska 2016)

$$T_s = BT/\{1+[(\lambda BT/\rho)*\ln\varepsilon]\} \quad (10)$$

Results and Discussion

The regions were analyzed based on the above data and formulas. Figure 1 below provides a descriptive analysis of the selected area on the Ustyurt Plateau according to the studied indices. It is advisable to perform the analysis using the statistical method (Jaksibaev, Aleuov 2020, Embergenov et al., 2020).

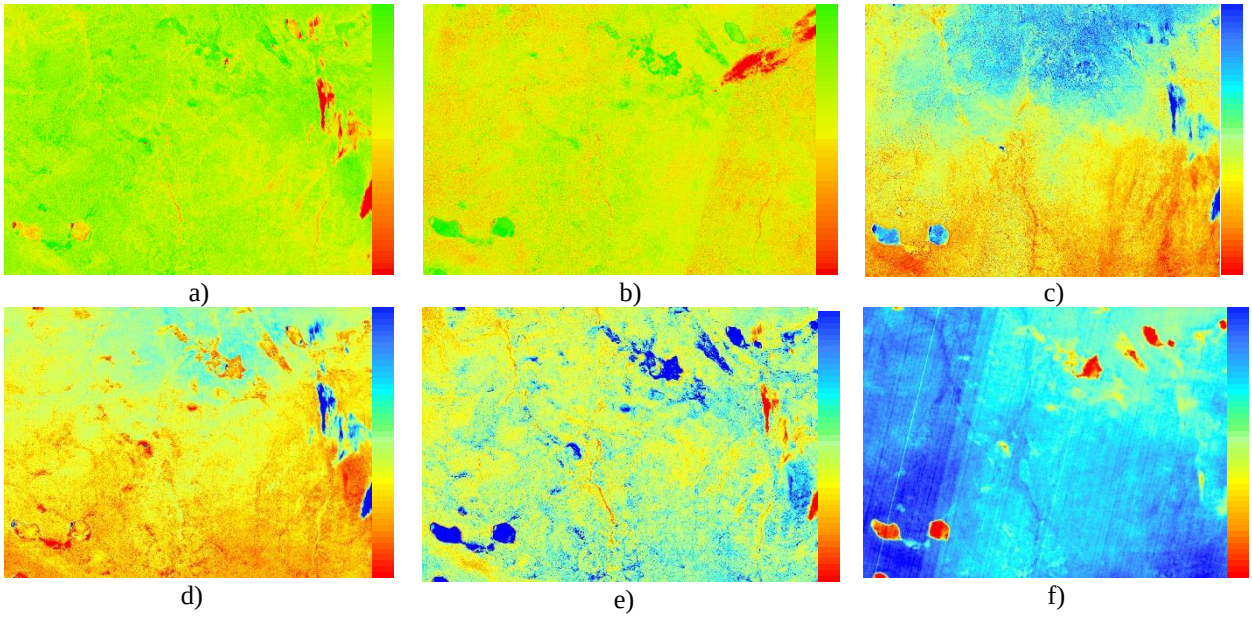

Figure 1. a) NDVI, b) BSI, c) NDWI, d) MNDWI, e) SI, f) LST (in October)

As can be seen from Figure 1 (a), we can see that the vegetation index is very low in the eastern part of this area and that there is a water source here (Figure 1 (c, d)). Figure 1 (e) shows the low salinity of this water source. But we can see places with high levels of salinity in the northeast and southwest of the region. Figure 1 (f) shows that areas with high salinity levels also have higher soil temperatures. This means that in areas with high salinity, the soil temperature will be higher.

The following analysis shows that the vegetation index varies from season to season. The highest vegetation index is reached in summer and early August. As the level of vegetation increases, bare soil index reaches a higher level. This indicates that there are plants in the area that grow in early spring and stop growing with the onset of summer, and that there is a lack of other plants instead of dry grass (Figure 2 (a)). But, the vegetation level in the area is very low. The water index peaks in winter and declines in spring and summer. This means that the evaporation rate in this area is very high (Figure 2 (b)). Figure 2 (c, d) shows that the highest salinity occurs in the summer and early August, and the soil temperature also peaks in August. This means that as the land surface temperature rises, so does the salinity of the earth's surface.

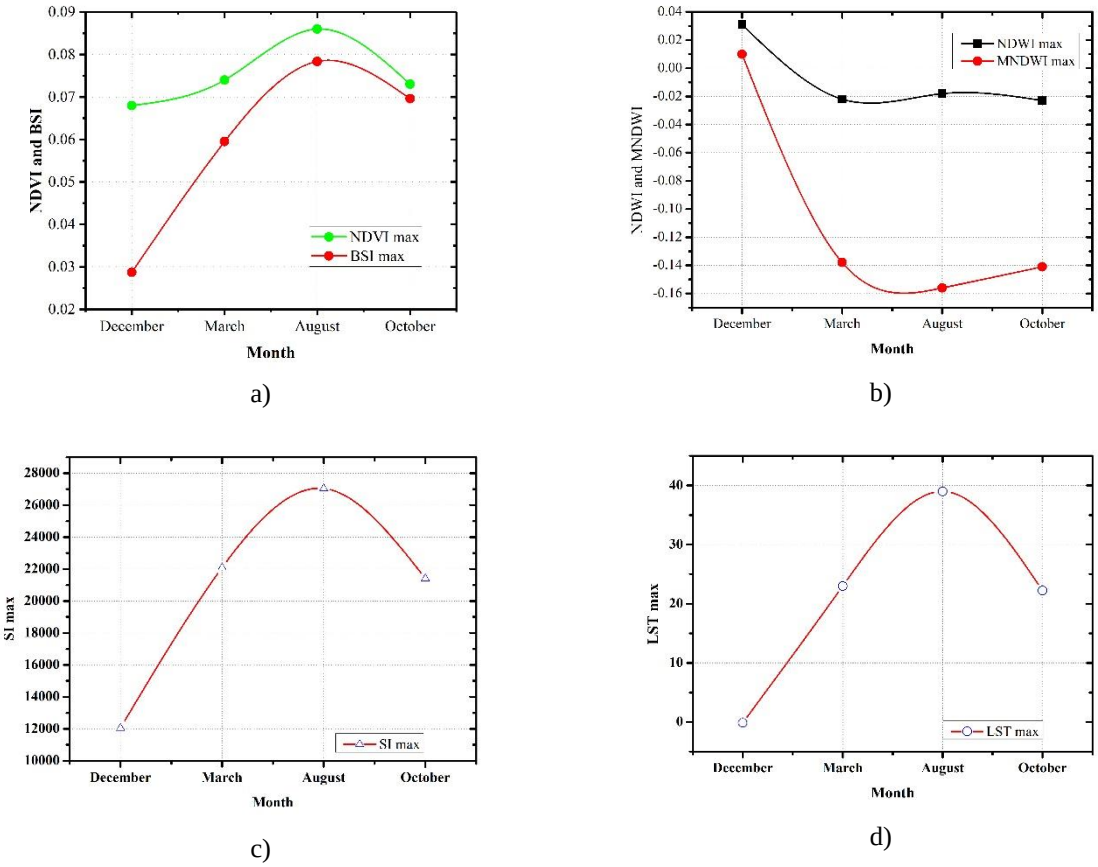

Figure 2. a) NDVI and NDBI, b) NDWI and MNDWI, c) SI, d) LST

Figure 2 below provides a descriptive analysis of the selected region from the Amudarya delta according to the studied indices. We can see high vegetation levels in the eastern and southern parts of the region (Figure 2 (a)). These areas have a high level of water supply. In the northwestern part, vegetation levels and water availability are very low (Figure 2 (a, c)) and salinity levels and land surface temperatures are very high (Figure 2 (e, f)). This means that in order for the vegetation level to be normal, the water supply level must be sufficient for the soil temperature and the salinity level must be low.

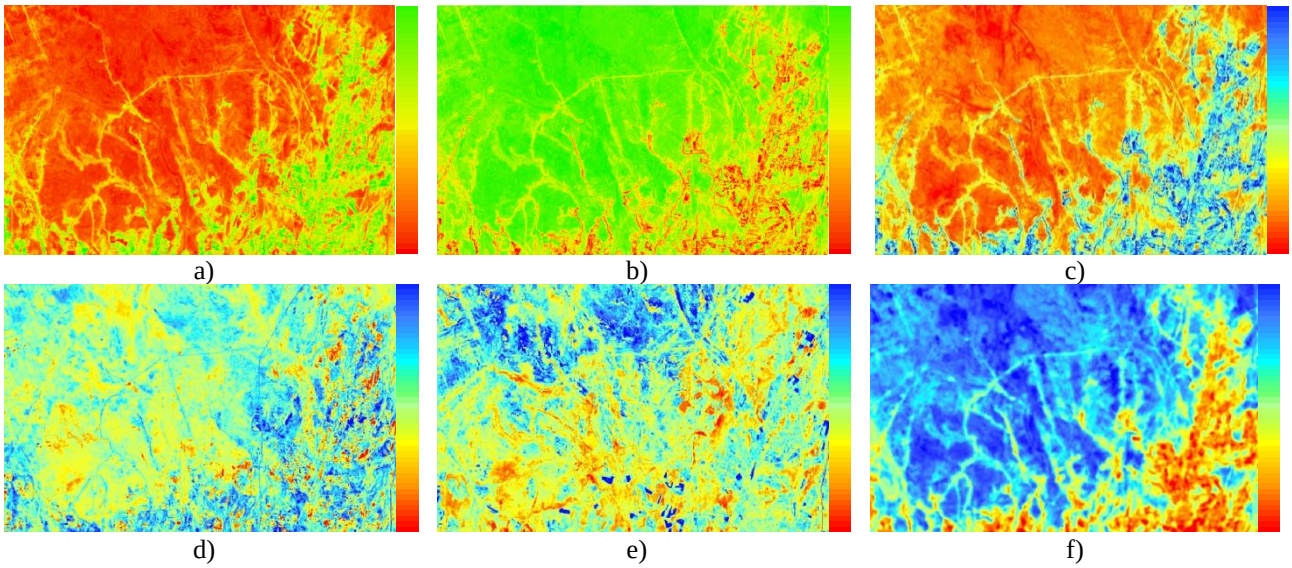

Figure 3.a) NDVI, b) BSI, c) NDWI, d) MNDWI, e) SI, f) LST (on August)

The vegetation index in this region also varies from season to season. The highest rates are in the summer and early August. We can see that the vegetation in this area belongs to different plants. Because of the bare soil index in the area remains unchanged during the intervals (Figure 4 (a)).

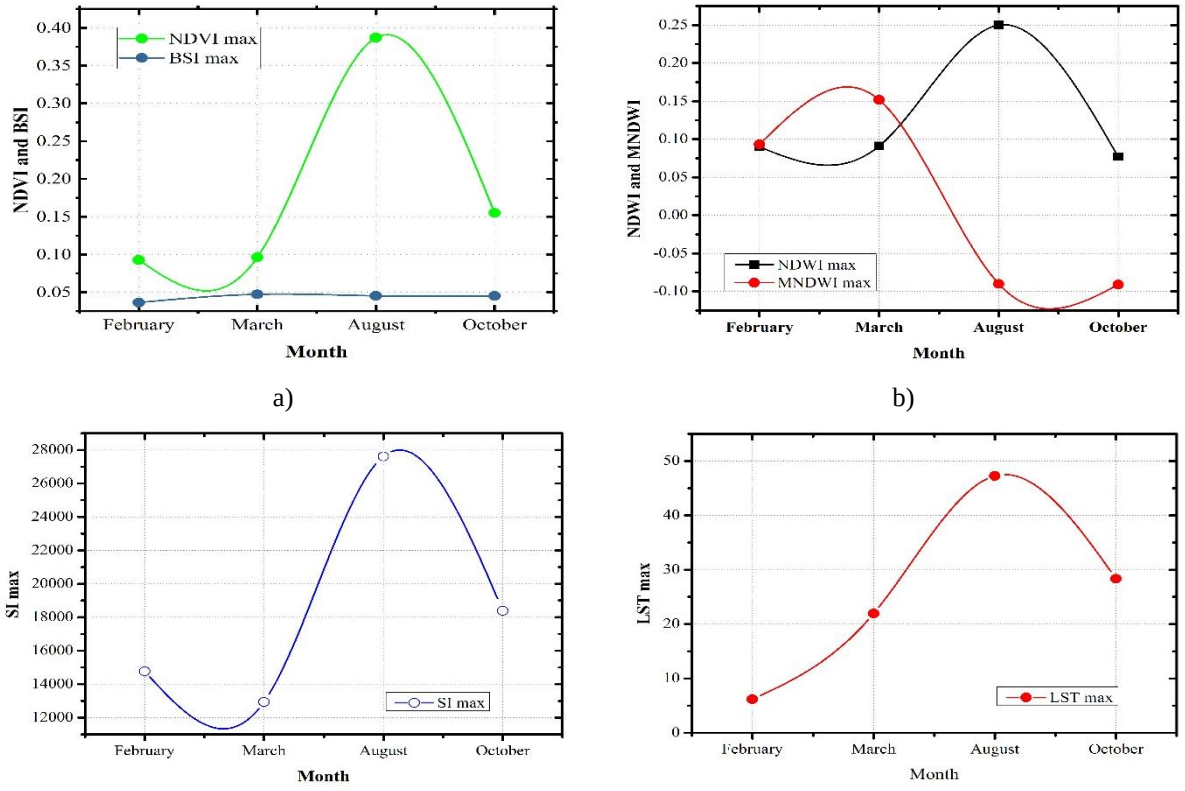

Figure 4.a) NDVI and NDBI, b) NDWI and MNDWI, c) SI, d) LST

The watershed rate is very low in August, but the water availability of plants is high (Figure 4 (b)). This means that there will be irrigated agriculture in the area. Salinity levels began to rise in early spring and peaked in August (Figure 4 (c)). Soil temperatures also peaked in August. The similarity of the processes taking place in both regions shows that the above assumptions are correct.

Conclusion

Based on the above data and analysis, we can see that land use around the Amudarya Delta is more efficient than on the Ustyurt Plateau. Because of the vegetation index was found to be very high in the area selected from the Amudarya delta (Figure 5 (a)). However, the salinity of the lands, which are increasing as a result of the drying up of the Aral Sea, is the same in both regions. The temperature difference in the northern and southern parts of Karakalpakstan is 28 days and the soil temperature in the selected area of the Amudarya delta is much higher and spring begins early, it is effective to use these lands as pastures in early spring (Figure 5 (b)) (Sultashova et al., 2021).

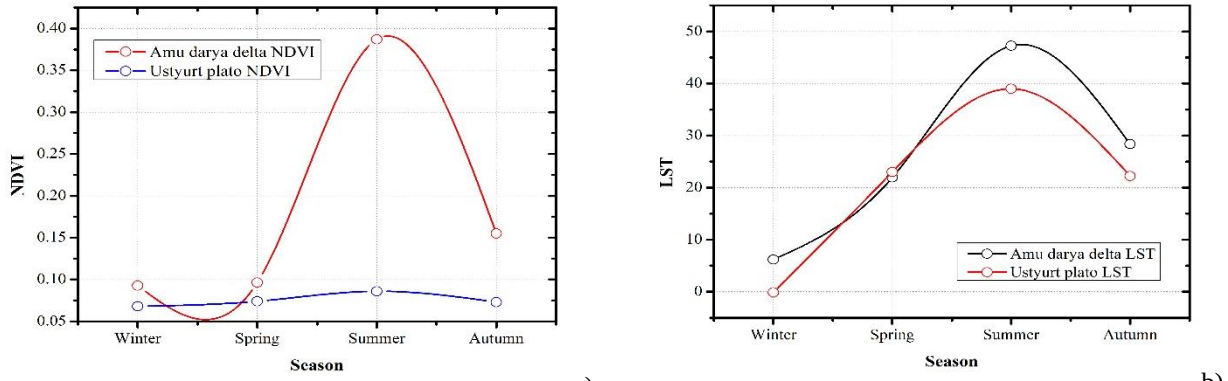

a) b)

Figure 5. a) NDVI, b) LST

References:

1. Avdan, U., & Jovanovska, G. (2016). Algorithm for Automated Mapping of Land Surface temperature Using LANDSAT 8 Satellite Data - Hindawi Publishing Corporation. *Journal of Sensors*, pages 8.
2. Berdimbetov, T.T., Ma, Z.-G.., Liang, C., & Ilyas, S. (2020). Impact of Climate Factors and Human Activities on Water Resources in the Aral Sea Basin. *Hydrology*, 7, 30. https://doi.org/10.3390/hydrology7020030
3. Can Trong Nguyen, Amnat Chidthaisong, Phan Kieu Diem and Lian-Zhi Huo (2021). A Modified Bare Soil Index to Identify Bare Land Features during Agricultural Fallow-Period in Southeast Asia Using Landsat 8. *Land*, 10, 231, 17 p. https://doi.org/10.3390/land10030231
4. Christopher Conrad, Muhammad Usman, Lucia Morper-Busch, Sarah Schönbrodt-Stitt (2020). Remote sensing-based assessments of land use, soil and vegetation status, crop production and water use in irrigation systems of the Aral Sea Basin. *Water Security* Volume 11, December, 11p., 100078. https://doi.org/10.1016/j.wasec.2020.100078
5. Di Bella, C., Faivre, R., Ruget, F., Seguin, B., Gue´ Rif, M., Combal, B., Weiss, M., & Rebella, C. (2004). Remote sensing capabilities to estimate pasture production in France. *International Journal of Remote Sensing*. Vol. 25, No. 23, 5359–5372. DOI: 10.1080/01431160410001719849. Pages 14.
6. Embergenov, N.J., Joldasov, A.S., & Oteuliev, M.O. (2020). Some issues of development of livestock sectors in the Republic of Karakalpakstan, *Jekonomika i socium*, №9(76), https://doi.org/10.46566/2225-1545_2020_76_22
7. (n.d.). Retrieved from https://www.gisgeography.com/ndvi-normalized-difference-vegetation-index
8. Turdimambetov, I., Pauditsova, E., Madreymov, A., Komilova, N., Oteuliev, M., Kayupov, N., Utarbaeva, K., & Eshimbetova, G. (2021). "Influence of harmful ecological factors on the population of the Republic of Karakalpakstan". *European Journal of Molecular & Clinical Medicine*, 7, 10, 2021, 1790-1796.
9. Jaksibaev, R.N. (2020) Determination of vegetation index, land surface temperature and precipitation amounts using remote sensing data. *Journal of Agro processing.* Volume 5. Issue 2, Pages 4-10. http://dx.doi.org/10.26739/2181-9904-2020-5-1
10. Jaksibaev, R.N., & Aleuov, A.S. (2020). Use of statistical methods in the analysis of land cover. *Electronic journal of Actual problems of modern science, education and training*, Volume 4, Pages 291-298. ISSN 2181-9750.
11. Oliveira, J., Campbell, E. E., Lamparelli, R. A.C., Figueiredo, G. K.D.A., Soares, J. R., Jaiswal, D., Monteiro, L. A., Vianna, M. S., Lynd, L. R., & Sheehan, J. J. (2020). Choosing pasture maps: An assessment of pasture land classification definitions and a case study of Brazil. *Int J Appl Earth Obs Geoinformation*, p.15, https://doi.org/10.1016/j.jag.2020.102205
12. Parente, L., & Ferreira, L. (2018). Assessing the Spatial and Occupation Dynamics of the Brazilian Pasturelands Based on the Automated Classification of MODIS Images from 2000 to

2016. *Remote Sens.*, 10, 606, Pages 14. doi:10.3390/rs10040606

13. Ji, L., Geng, X., Sun, K., Zhao, Y., & Gong, P. (2015). Target Detection Method for Water Mapping Using Landsat 8 OLI/TIRS Imagery. *Water*, 7, 794-817. doi:10.3390/w7020794 Pages 794-817.
14. Legg, M., & Bradley, S. (2020). Ultrasonic Arrays for Remote Sensing of Pasture Biomass. *Remote Sens.*, 12(1), 111. https://doi.org/10.3390/rs12010111
15. Elhag, M. (2015). Evaluation of Different Soil Salinity Mapping Using Remote Sensing Techniques in Arid Ecosystems, Saudi Arabia. *Journal of Sensors*, Article ID 7596175, 8 pages http://dx.doi.org/10.1155/2016/7596175.
16. Pereira, O. J. R., Ferreira L. G., Pinto, F., & Baumgarten, L. (2018). Assessing Pasture Degradation in the Brazilian Cerrado Based on the Analysis of MODIS NDVI Time-Series. *Remote Sens.*, 10, 1761, Page 14. doi:10.3390/rs10111761
17. Diek, S., Fornallaz, F., & Michael, E. (2017). Schaepman and Rogier de Jong. Barest Pixel Composite for Agricultural Areas Using Landsat Time Series. *Remote sensing*, Pages 31. Doi 10.3390/rs9121245.
18. Sultashova, O., Khudaybergenov, Ya., Oteuliev, M., & Reimov, M. (2020). Modeling of Temperature Mode of the Soil, *International Journal of Psychosocial Rehabilitation*, 24(4), pp. 6057-6068. https://doi.org/10.37200/IJPR/V24I4/PR2020416
19. Sultashova, O.G., Jaksibaev, R.N., & Aleuov, A.S. (2021). Dangerous meteorological events affecting pasture plants in Karakalpakstan. *Jekonomika i socium*, №5(84), p. 7.
20. Turdimambetov, I., Madreymov, A., Foldvary, L., Oteuliev, M., Kurbanov, M., Utarbaeva, K., & Bekanov, K. (2021). Influence of adverse ecological factors on the incidence of malignant neoplasms. *E3S Web of Conferences.* Volume 227, 6 January 2021, Article number 02001. E3S Web Conf., 227 (2021) 02001. DOI: https://doi.org/10.1051/e3sconf/202122702001
21. Turdimambetov, I. R., Oteuliev, M. O., & Karimbaev, Q. K. (2021). The current state of medical service in the quality of life of the population of the Republic of Karakalpakstan. *ISJ Theoretical & Applied Science*, 04 (96), 262-267. Soi: http://s-o-i.org/1.1/TAS-04-96-54 Doi: https://dx.doi.org/10.15863/TAS.2021.04.96.54
22. Norqulov, U., & Sheraliev, H. (2010). *Yaylovlar melioratsiyasi.* (p.160). Toshkent: Yangi asr avlodi.